Rev. Roum. Sci. Techn.– Électrotechn. et Énerg.
Vol. **64**, *1*, pp. 45–50, Bucarest, 2019

SOURCE CURRENT HARMONICS SUPPRESSION IN DOMESTIC INDUCTION HEATER

AVIJIT CHAKRABORTY[1], ARIJIT CHAKRABARTI[1], PRADIP KUMAR SADHU[2]

Keywords: Asymmetrical-voltage-cancellation (AVC), Induction heating system, Insulated gate bipolar transistor (IGBT), Low pass filter (LPF), Power-simulator (PSIM), Total harmonic distortion (THD).

This paper aims at searching for the application of a ring type passive low pass filter (LPF) to reduce the entry of undesired harmonics to the input source from the inverter side of a full-bridge inverter based induction heating systems. The low pass filter is placed in between the ac input voltage source and high frequency full-bridge inverter based domestic induction heater. The inverter circuit is realized with insulated gate bipolar junction transistors (IGBT) as main power electronic switches. Unwanted harmonics are produced in the system due to non-linear behavior of the load under the effect of the power semi-conductor switches, which make the source current waveform non-sinusoidal. In this paper, the induction heating system is subjected to asymmetrical voltage cancellation (AVC) control and fast Fourier transform (FFT) method is utilized for frequency domain analysis to realize influence of harmonics. The whole system is implemented in power simulator (PSIM) environment. It is found that the proposed filter can decrease the total harmonic distortion (THD) and increase the distortion factor (DF) of the input current. Moreover, it is also proved that the can also improve the input power factor.

1. INTRODUCTION

In recent years, induction heating process is gradually becoming a very popular and well accepted technical process to generate very quick heat in a controllable manner in various appliances like domestic cooking, steel melting, brazing, etc. [1]. It is regarded as a very fast contact free heating method that is free from any carbon dioxide (CO_2) emission and thus does not cause any hazard to the environment. The most essential and inseparable part of any induction heating system is the resonant Inverter, operating as very high frequency ac current generator. Various topological circuits are so far proposed for these high frequency resonant inverters such as single switch quasi-resonant [2], the half-bridge inverter [3, 10], full-bridge inverter [4, 5, 11, 12], hybrid inverter [6] etc.

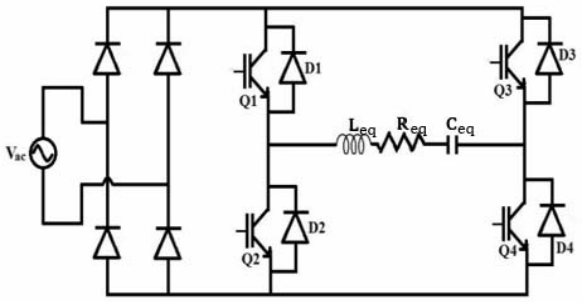

Fig. 1 – Full-bridge series resonant induction heating system.

Any induction heating system requires an ac input source, which must deliver a pure sinusoidal voltage and current at its input terminals. But due to non-linear behaviour of the load and the presence of power electronic non-linear switching devices, harmonics are produced within the induction heating system. These harmonics distort the input source current and put adverse effects on the normal operation of the system. Active and passive filters with suitable designs are so far proposed for harmonics eliminations in different electrical systems [7, 8]. In this paper, the effect of a ring type passive filter is discussed which is applied to an asymmetrical voltage cancellation (AVC) controlled full-bridge inverter. It will be shown that the input ac source current becomes almost purely sinusoidal after successful harmonics suppression to a great extent. Furthermore, the proposed filter can also provide wider range of power control and will also make the input power factor almost nearly equal to unity ensuring low reactive power insertion from the ac source.

2. OPERATIONAL PRINCIPLE OF THE INDUCTION HEATING SYSTEM

In Fig. 1, the proposed full-bridge inverter based induction heating system is shown. It carries a series resonant load consisting of an equivalent resistor R_{eq}, equivalent inductor L_{eq} and resonant capacitor C_{eq}. Total four IGBTs (Q1-Q4) along with anti-parallel diodes (D1-D4) provide the path for the load current such that each diode provides the path for reverse conduction of the load current during freewheeling period. Each IGBT is switched on following the conduction of its corresponding anti-parallel diode ensuring zero voltage switching (ZVS) condition during turn-on.

In this induction heating system, at the initial stage, the line frequency of 50 Hz ac supply voltage is rectified to dc voltage by a full-bridge uncontrolled rectifier unit. After that a dc link capacitor connected parallel smoothens this rectified dc voltage, which is later, applied to the input of a full-bridge series resonant inverter to produce very high frequency current. This high frequency current is sent through an inductor coil and creates very high frequency magnetic field and this magnetic field while penetrating the working load generates heat.

The impedance of the induction-heating load can be represented as follows

[1]Research Scholar in Electrical Engineering Department, Indian Institute of Technology (Indian School of Mines), Dhanbad - 826004, India, E-mail: ab.chakt@gmail.com
[2]Electrical Engineering Department, Indian Institute of Technology (Indian School of Mines), Dhanbad - 826004, India.

$$Z_{eq} = R_{eq} + \mathrm{j}X_{eq} = R_{eq} + \mathrm{j}\left(\omega_s L_{eq} - \frac{1}{\omega_s C_{eq}}\right)$$
$$= R_{eq} + \mathrm{j}\left(\Omega Q_l R_{eq} - \frac{1}{\Omega} Q_l R_{eq}\right) \quad (1)$$
$$= R_{eq}\left[1 + \mathrm{j}Q_l\left(\Omega - \frac{1}{\Omega}\right)\right].$$

Here, the magnitude and the phase angle can be written as follows

$$\left|Z_{eq}\right| = R_{eq}\sqrt{1 + Q_l^2\left(\Omega - \frac{1}{\Omega}\right)^2} \quad (2)$$

$$\phi = \tan^{-1}\left\{Q_l\left(\Omega - \frac{1}{\Omega}\right)\right\}, \quad (3)$$

where

$$\Omega = \frac{\omega_s}{\omega_o} \quad (4)$$

is the normalized switching frequency, and

$$\omega_o = \frac{1}{\sqrt{L_{eq}C_{eq}}} \quad (5)$$

is representing the resonant angular frequency. $\omega_s = 2\pi f_s$ is the angular switching frequency and f_s is switching frequency and moreover the quality factor of the load is given by following equation

$$Q_l = \frac{\omega_o L_{eq}}{R_{eq}} = \frac{1}{\omega_o R_{eq} C_{eq}}. \quad (6)$$

3. ASYMMETRICAL VOLTAGE CANCELLATION (AVC) CONTROL

It is admired as one of reliable fixed frequency control technique, which can be applied for wide range power control maintaining the zero voltage switching (ZVS) condition during both turn-on and turn-off conditions. In AVC control technique [9], the voltage waveform is fixed to zero value on either side asymmetrically and the duration of this zero value is continuously regulated for output power control. The three basic control parameters are α_+, α_- and β respectively as shown in Fig. 2.

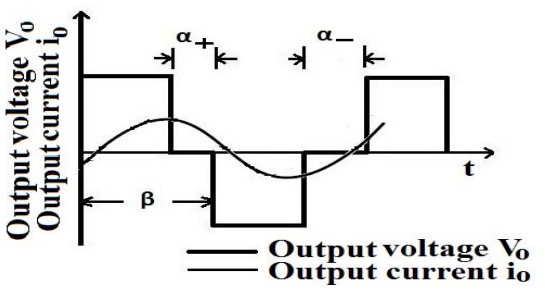

Fig. 2 – Output voltage and current waveform under AVC control.

Applying the Fourier series, the magnitude and the phase of the k^{th} harmonic component of the output voltage V_o can be expressed by the following equations

$$V_{ok} = \frac{V_{dc}}{k\pi}\sqrt{a_k^2 + b_k^2}, \quad (7)$$

$$\phi_{ok} = \tan^{-1}\frac{a_k}{b_k}, \quad (8)$$

where

$$a_k = \left[\sinh k(\beta - \alpha_+) + \sinh k\beta + \sinh k\alpha_-\right] \quad (9)$$
$$b_k = \left[1 - \cosh k(\beta - \alpha_+) - \cosh k\beta + \cosh k\alpha_-\right]. \quad (10)$$

The output power using AVC control can be expressed as

$$P_o = \frac{V_{o1}^2}{2R_{eq}\left[1 + Q_l^2\left(\Omega - \frac{1}{\Omega}\right)^2\right]}, \quad (11)$$

while considering only the fundamental component for $k = 1$.

To obtain the optimum control from the AVC control method, it is better to select the values of the control parameters such as $\alpha = \alpha_+$, $\alpha_- = 0^\circ$ and $\beta = 180^\circ$.

Then, the fundamental output voltage magnitude and phase can be expressed by the following equations

$$V_{o1} = \frac{V_{dc}}{\pi}\left[10 + 6\cos\alpha\right]^{\frac{1}{2}}, \quad (12)$$

$$\phi_{o1} = \tan^{-1}\left[\frac{\sin\alpha}{3 + \cos\alpha}\right]. \quad (13)$$

Moreover, the maximum output voltage V_{o1m} and maximum output power P_{o1m} can be obtained if $\alpha_+ = 0^\circ$ and $\beta = 180^\circ$ as below

$$V_{o1m} = \frac{4V_{dc}}{\pi}, \quad (14)$$

$$P_{o1m} = \frac{V_{o1m}^2}{2R_{eq}\left[1 + Q_l^2\left(\Omega - \frac{1}{\Omega}\right)^2\right]}. \quad (15)$$

Due to the inductive nature of the load, the load current i_o is lagging behind V_{o1} by a certain angle as given below

$$\phi_1 = \tan^{-1}\left[\frac{\left(\Omega^2 - 1\right)Q_l}{\Omega}\right]. \quad (16)$$

Besides, the representation of the normalized output voltage and the normalized output power can be made by the following equations

$$v = \frac{V_{o1}}{V_{o1m}} = \frac{\left[10 + 6\cos\alpha\right]^{\frac{1}{2}}}{4}, \quad (17)$$

$$p = \frac{P_{o1}}{P_{o1m}} = \left(\frac{V_{o1}}{V_{o1m}}\right)^2 = \frac{5 + 3\cos\alpha}{8}. \quad (18)$$

It is desirable that each IGBT must operate under ZVS condition to achieve minimum switching loss and for doing this the following condition has to be satisfied

$$\phi_1 - \phi_{o1} > 0,$$

$$\text{or } \frac{\left(\Omega^2-1\right)Q_l}{\Omega} > \frac{\sin\alpha}{3+\cos\alpha}. \quad (19)$$

For any IGBT, with AVC control technique, ZVS turn-on occurs whenever its corresponding the anti-parallel diode conducts negative current prior the turning-on of that IGBT. The output voltage is positive while either D1–D4 or Q1–Q4 for the first leg of the inverter conducts. Similarly, the output voltage becomes negative while either D2–D3 or Q2–Q3 for the second leg of the inverter conducts. Moreover, the output voltage becomes zero if any two switches from each leg conduct simultaneously.

4. PROPOSED PASSIVE FILTER

In Fig. 3, the circuit diagram of the proposed ring filter is presented, which consists of two inductors each of value L and two capacitors each of value C. Both inductors block the flow of high frequency ac current components from the source side to the inverter side and similarly also block the flow of very high frequency ac current components from the inverter side to the source side. On the other hand, the left and the right handed capacitors block the flow of high frequency ac voltage ripples from the source and inverter sides respectively.

The equivalent value of the reactance of this network from the source side can be expressed as follows

$$X = \frac{\frac{2L}{C}-\frac{1}{\omega^2}}{2\,\mathrm{j}\left(\omega L-\frac{1}{\omega C}\right)}. \quad (20)$$

From above equation, X will be very high if

$$\omega = \omega_1 = \frac{1}{\sqrt{LC}}. \quad (21)$$

Here, L= 200 μH and C= 0.1 μF and thus the cut-off frequency for this filter is f_1= 35.6 kHz and it has the ability to block the high frequency current waveform with fundamental frequency of 40 kHz, which is the fundamental frequency of the output or load current.

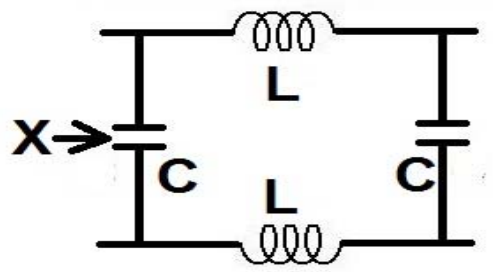

Fig. 3– Circuit diagram of the ring filter.

5. TOTAL HARMONIC DISTORTION (THD)

Total harmonic distortion is regarded as a very significant measuring parameter that gives an indication of how close the shape of a periodic non-sinusoidal waveform to its fundamental component This is an index to visualize the effect of harmonic components present in a non-sinusoidal waveform and the degree of deviation of the waveform with respect to its fundamental component.

In terms of current, THD can be expressed as follows

$$\mathrm{THD} = \frac{\sqrt{\sum_{k=2,3,\ldots}^{k} I_{nrms}^2}}{I_{1rms}}. \quad (22)$$

Here, I_{1rms} = root mean square (RMS) value of the fundamental component and I_{krms} = RMS value of the k^{th} harmonic. A greater THD value of a certain waveform provides the indication of greater distortion of that waveform from the fundamental component.

6. DISTORTION FACTOR (DF)

Distortion factor is regarded as another parameter to indicate the harmonics level to be present in any periodic waveform, after the waveform is subjected to 2^{nd} order attenuation (*i.e.* divided by k^2), where, k = 1, 2, 3, etc. It is represented by the mathematical equation as follows

$$\mathrm{DF} = \frac{\sqrt{\sum_{k=2,3,\ldots}^{k}\left(\frac{I_{krms}}{k^2}\right)^2}}{I_{1rms}} \quad (23)$$

High value of the distortion factor indicates the presence of greater amount of harmonics in the waveform.

7. SIMULATION RESULTS

To verify the effect of the proposed passive filter on the input ac supply voltage waveform, the proposed series resonant full-bridge inverter is operating with a switching frequency of 40 kHz and the ac supply voltage is 230 V. The equivalent parameters of the induction heating load are R_{eq} = 1 Ω and L_{eq} = 50 μH respectively. Moreover, the common resonant capacitor C_{eq} has the value of 0.6 μF.

The effect of the proposed filter is analyzed through power system simulator (PSIM) software. The effect is first verified without inserting the filter and then it is verified after inserting the filter. The total harmonic distortion (THD), distortion factor (DF) and input power factor (IPF) of the induction heater is determined for each case separately.

8. THD, DF, IPF CALCULATION OF THE INDUCTION HEATER IN THE ABSENCE OF THE FILTER

In Fig.4, the PSIM circuit diagram of the proposed induction heater without incorporating the filter. Figure 5 shows the waveform of the input current of the induction heating system without inserting the proposed passive filter. Fig. 6 is showing the positive half-cycle of the same waveform and finally the fast Fourier transform (FFT) spectrum of the input ac current is depicted in Fig. 7. All these waveforms are obtained through PSIM simulations.

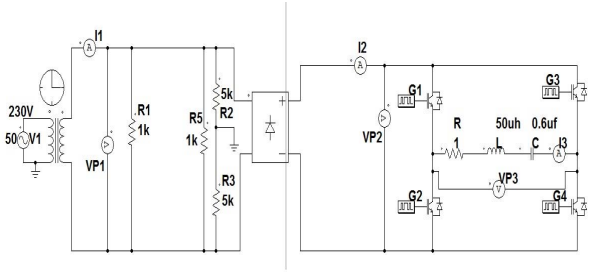

Fig. 4 – PSIM circuit diagram of the induction heating system without filter.

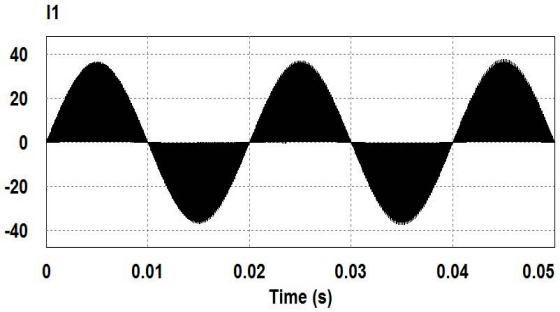

Fig. 5 – Input current waveform without filter for α = 30º.

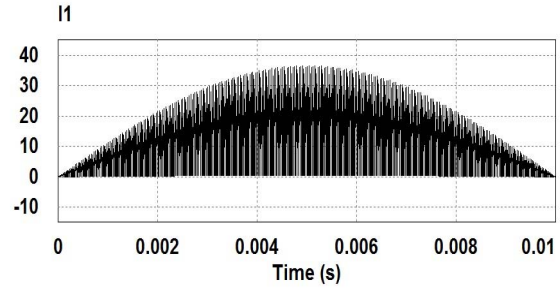

Fig. 6 – Input current waveform without filter for α = 30º for the positive half-cycle.

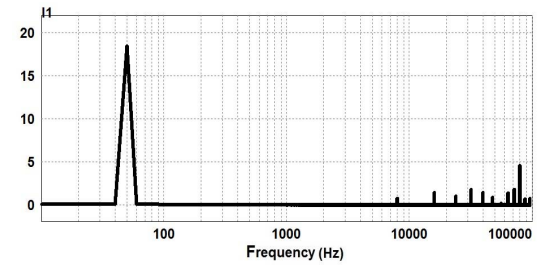

Fig. 7 – FFT spectrum of the input current waveform without filter for α=30º (Ampere in X axis and logarithmic scale in Y axes.).

Table I
Parameter Variation without Filter

Control angle (α) in degrees	THD of the input source current (%)	Output power (P_o) in watts	Input power factor ($\cos\theta_i$)	Distortion factor (μ)
30	61.55	1467	0.875	0.85
40	59.66	1050	0.822	0.86
50	77.06	978	0.796	0.79
60	75.31	1183	0.863	0.80
70	74.08	878	0.765	0.80
80	73.34	892	0.757	0.81
90	73.05	879	0.807	0.81
100	91.15	865	0.758	0.74

Table I shows the variation of the THD, output power P_o, input power factor (IPF) and distortion factor with respect to the control angle α of the induction heater without inserting the filter.

9. THD, DF, IPF CALCULATION OF THE INDUCTION HEATER IN THE PRESENCE OF THE FILTER

In Fig.8, the PSIM circuit diagram of the proposed induction heater after inserting the filter. Fig. 9 shows the waveform of the input current of the induction heating system without inserting the proposed passive filter. Fig. 10 is showing the positive half-cycle of the same waveform and finally the Fast Fourier Transform (FFT) spectrum of the input ac current is depicted in Fig. 11. All these waveforms are obtained through PSIM simulations.

Table II shows the variation of the THD, output power P_o, input power factor (IPF) and distortion factor with respect to the control angle α of the induction heater after inserting the filter.

Table II
Parameter variation with filter

Control angle (α) in degrees	THD of the Input source current (%)	Output power (P_o) in watts	Input power factor ($\cos\theta_i$)	Distortion factor (DF) (μ)
30	5.92	1915	0.997	0.99
40	10.26	1625	0.995	0.99
50	10.63	1285	0.995	0.99
60	12.21	1099	0.993	0.99
70	14.53	1012	0.988	0.98
80	16.44	946	0.987	098
90	23.26	716	0.973	0.97
100	26.14	625	0.969	0.96

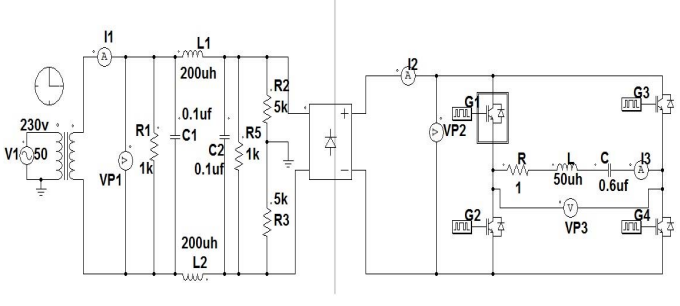

Fig. 8 – PSIM circuit diagram of the induction heating system with filter.

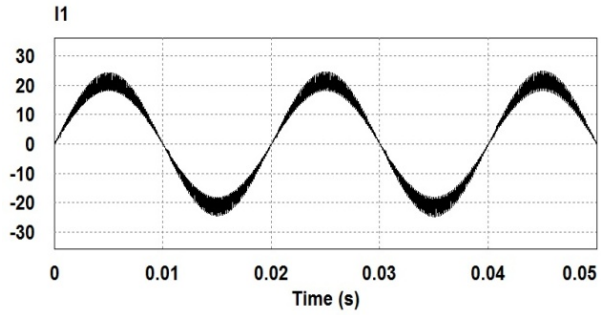

Fig. 9– Input current waveform with filter for α =30°.

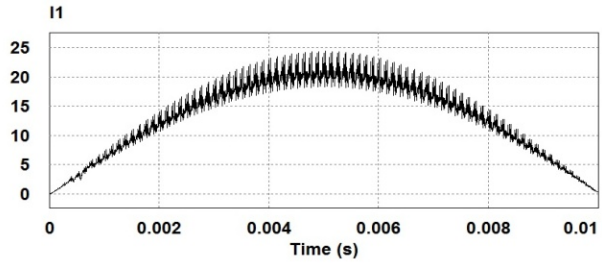

Fig. 10– Input current waveform with filter for α =30° for the positive half-cycle.

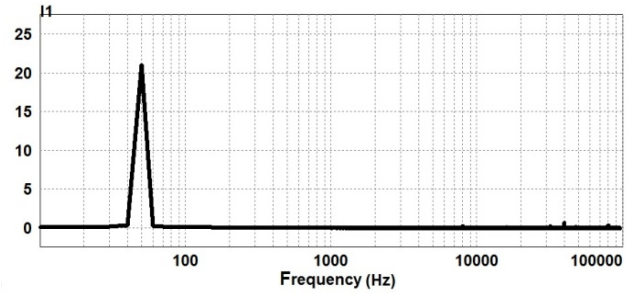

Fig. 11 – FFT spectrum of the input current waveform with filter for α =30° (Ampere in X axis and logarithmic scale in Y axes).

10. RESULTS AND DISCUSSION

From the PSIM simulations of the circuits shown in Fig. 4 and Fig. 8 of the proposed induction heater, two distinct results are achieved. Fig. 5 is showing the input current waveform without using the passive filter for the phase angle α=30°, which has a non-sinusoidal shape indicating a greater amount of harmonics presence in it due to very high frequency switching operations (switching frequency f_s= 40 kHz). The presence of these very high frequency harmonics can be more prominently observable in the same input current waveform in the positive half-cycle for the phase angle α=30° as depicted in Fig. 6. Due to the absence of passive filter, it is found that, in the FFT waveform represented in logarithmic scale (in ampere in the X axis and in logarithmic scale in the Y axes as obtained from PSIM simulation) as shown in Fig. 7 of the input current from the source contains very high frequency harmonics which has the fundamental frequency of f_1= 40 kHz. So, the input current waveform of supply frequency f = 50 Hz is largely affected by the very high frequency harmonics having fundamental frequency of f_1= 40 kHz due to the high frequency switching operations of the inverter. Similarly, from Table I, higher THD values and lower distortion factor (DF) value significantly indicate that the input current waveform is largely affected by the high frequency harmonics over the entire range of α. Meanwhile, Fig. 9 is showing the input current waveform using the passive filter for the phase angle α=30°, which has a wave shape almost nearly sinusoidal in nature. The closeness of the shape of this waveform to sinusoidal in nature indicates a very less amount of harmonics presence produced due to very high frequency switching operations of the inverter. It can be more prominently visible in Fig. 10.for the positive half-cycle, in which the high frequency harmonics level is greatly reduced. Besides, in the FFT waveform (represented in ampere in the X axis and in logarithmic scale in the Y axes) of the input current as shown in Fig. 11, the presence of very high frequency harmonics due to high frequency switching operations is reduced significantly. Also, the identical result is shown in Table II, in which the THD values are greatly reduced and distortion factor (DF) values are increased over the entire range of α. Moreover, from Table I and Table II, it is quite clear that the output power control range is significantly increased when the induction heater incorporates the passive filter.

Also, the use of filter increases the input power factor closer to unity as presented in Table II for each value of α indicating relatively less reactive power injection from input source side which keeps the magnitude of the input current from the source to a relatively lower value for a certain output power and results less conduction loss with more efficient operation. This ring filter as a result can thus provide various advantages and thus can be used in other applications also.

11. CONCLUSION

In this paper, the harmonics effect present in the input ac current is investigated for a very high frequency series resonant inverter based induction heater with and without utilizing a passive filter. In the former case, without the filter, the large THD value and relatively lower DF value of the input current indicate the presence of high degree of harmonic level and at the same time the low input power factor (IPF) represents entry of greater amount of reactive power from the line frequency supply. In the later case, when the proposed filter is inserted properly, then the THD of the input source current reduces drastically to a low value and DF increases to a relatively higher value for all values of the control angle α and hence reduces the degree of the harmonic level of the input current by suppressing the harmonics comprehensively and moreover, in the second case, too, the input power factor is improved to a larger value leading less reactive power injection from the input supply.

ACKNOWLEDGEMENTS

Authors wish to thank the UNIVERSITY GRANTS COMMISSION, India for granting the financial support under Major Research Project entitled “Simulation of high frequency mirror inverter for energy efficient induction heated cooking oven using PSPICE” and also they are grateful to the Under Secretary and Joint Secretary of UNIVERSITY GRANTS COMMISSION, India for their active co-operation.

Received on July 22, 2017

REFERENCES

1. O. Lucía, P. Maussion, E. J. Dede, J. M. Burdío, *Induction Heating Technology and Its Applications: Past Developments, Current Technology, and Future Challenges,* IEEE Transactions on Industrial Electronics, **61**, *5*, pp. 2509–2520 (2013).
2. A. Chakraborty, P. K. Sadhu, K. Bhaumik, P. Pal, N. Pal, *Behaviour of a High Frequency Parallel Quasi Resonant Inverter Fitted Induction Heater with Different Switching Frequencies*, International Journal of Electrical and Computer Engineering, **6**, *2*, pp. 447–457 (2016).
3. Y. S. Kwon, S. B. Yoo, D. S. Hyun, *Half Bridge series resonant inverter for induction heating applications with load adaptive PFM control strategy*, in Proc. IEEE Power Electronics Conference Andex position (APEC), **l**, pp. 575–581 (1999).
4. A. Chakraborty, D. Roy, T. K. Nag, P. K. Sadhu, N. Pal, *Open Loop Power Control of A Two-Output Induction Heater,* Rev.Roum. Sci. Techn. – Électrotechn. et Énerg., **62**, *1*, pp. 48–54 (2017).
5. V. V. S. K. Bhajana, P. Drabek, M. Jara, *Performance Evaluation of LLC Resonant Full Bridge DC Converter for Auxiliary Systems in Traction*, Rev.Roum. Sci. Techn. – Électrotechn. et Énerg., **60**, *1*, pp. 79–88 (2015).
6. A. Bhattacharya, P. K. Sadhu, A. Bhattacharya, N. Pal, *Voltage Controlled Resonant Inverter- An Essential Tool For Induction Heated* Equipment, Rev.Roum. Sci. Techn. – Électrotechn. et Énerg., **61**, *3*, pp. 273–277 (2016).
7. B. Singh, K. Al-Hadad, A. Chandra, *A Review of Active Filters for Power Quality Improvement*, IEEE transactions on Industrial Electronics, **46**, 5, pp. 960– 971, (1999).
8. P. A. Dahano, A. Purwadi, Q. Amaruzzaman, *An LC Filter Design Method for Single-Phase PWM inverters*, Power Electronics and Drive Systems, **2**, pp. 571–576 (1995).
9. J. M. Burdio, L. A. Barragan, F. Monterde, D. Navarro, J. Acero, *Asymmetrical Voltage-Cancellation Control for Full-Bridge Series Resonant Inverters,* IEEE Transactions on Power Electronics, **19**, *2*, pp. 461–469 (2004).
10. A. Chakraborty, P. K. Sadhu, A. Chakrabarti, A. Basak, N. Pal, *Asymmetrical Duty Cycle Phase-Shifted Dual Output Induction Cooker*, Rev.Roum. Sci. Techn. – Électrotechn. et Énerg., **63**, *1*, pp. 65–70 (2018).
11. A. Chakrabarti, P. K. Sadhu, A. Chakraborty, P. Pal, *Brain Emotional Learning Based Intelligent Controller for Induction Heating Systems*, Rev.Roum. Sci. Techn. – Électrotechn. et Énerg., **63**, *1*, pp. 58–64 (2018).
12. A. Chakrabarti, A. Chakraborty, P. K. Sadhu, *A Fuzzy Self-Tuning PID Controller with a Derivative Filter for Power Control in Induction Heating Systems*, Journal of Power Electronics, **17**, *6*, pp. 1577–1586 (2017).